# A new dynamo pattern revealed by the tilt angle of bipolar sunspot groups

A Tlatov<sup>1</sup>\*, E. Illarionov<sup>2</sup>†, D. Sokoloff<sup>3</sup>‡, V. Pipin<sup>4</sup>§

- <sup>1</sup>Kislovodsk Mountian Astronomical Station of the Pulkovo Observatory, 357700, Box-145, Kislovodsk, Russia
- <sup>2</sup>Department of Mechanics and Mathematics, Moscow State University, Moscow,119991, Russia
- <sup>3</sup>Department of Physics, Moscow State University, Moscow,119992, Russia
- <sup>4</sup>Institute of Solar-Terrestrial Physics, Russian Academy of Sciences, Irkutsk, 664033, Russia

27 ноября 2021 г.

#### ABSTRACT

We obtain the latitude-time distribution of the averaged tilt angle of solar bipoles. For large bipoles, which are mainly bipolar sunspot groups, the spatially averaged tilt angle is positive in the Northern solar hemisphere and negative in the Southern, with modest variations during course of the solar cycle. We consider the averaged tilt angle to be a tracer for a crucial element of the solar dynamo, i.e. the regeneration rate of poloidal large-scale magnetic field from toroidal. The value of the tilt obtained crudely corresponds to a regeneration factor corresponding to about 10% of r.m.s. velocity of solar convection. These results develop findings of Kosovichev and Stenflo (2012) concerning Joy's law, and agree with the usual expectations of solar dynamo theory. Quite surprisingly, we find a pronounced deviation from these properties for smaller bipoles, which are mainly solar ephemeral regions. They possess tilt angles of approximately the same absolute value, but of opposite sign compared to that of the large bipoles. Of course, the tilt data for small bipoles are less well determined than those for large bipoles; however they remain robust under various modifications of the data processing.

**Key words:** Solar activity – solar magnetic fields – solar dynamo

# 1 INTRODUCTION

There is a widely accepted idea that the solar magnetic activity, which is itself manifested in the quasiperiodic variation of sunspot number and other similar tracers, results from the dynamo waves of quasistationary magnetic field propagating in solar interior. Differential rotation which stretches the toroidal magnetic field from poloidal is an obvious driver for the solar dynamo. Differential rotation alone is not capable of exciting the dynamo. Additional drivers which can create poloidal fields from toroidal ones are required. Symmetry arguments brought Parker (1955) to the idea that the collective action of the cyclonic motions (associated with the  $\alpha$ -effect) in the solar convection zone can transform the toroidal component of the large-scale magnetic field to poloidal. Steenbeck, Krause and Rädler (see Krause and Rädler, 1980) provided the mathematical basis for this idea. It was found that

the  $\alpha$ -effect results from the breaking of the reflection symmetry of the convective flows due to the global rotation. Currently, several different kinds of  $\alpha$ -effect are widely used in solar dynamo models. The flux-transport and the Babcock-Leighton types of dynamo employ a nonlocal  $\alpha$ effect, which results from the Coriolis force acting on flux-tubes rising in the solar convection zone (see, e.g., Choudhuri et al. 1995; Dikpati and Charbonneau 1999). They show that this kind of dynamo can operate in the Sun in conjunction with meridional circulation. In mean-field dynamos the  $\alpha$ -effect works in situ. It is more then plausible (Dikpati and Gilman, 2001) that both effects contribute to solar dynamo action, and their relative importance differs between normal cycles and the Grand Minimum epochs. Anyway, the physical nature of the dynamo driver which connects toroidal magnetic field with poloidal remains an important problem in solar dynamo theory.

Helioseismology provides a substantial observational basis which can illuminate the properties of the solar rotation. The driver of the poloidal magnetic field in the solar dynamo is much less well known than the differential rotation which largely drives the toroidal field, because

\* email: tlatov@mail.ru

† email: egor.mypost@gmail.com ‡ email: sokoloff.dd@gmail.com

§ email: pip@iszf.irk.ru

it is weaker and requires more sophisticated observational schemes. Seehafer (1990) suggested that the current helicity in solar active regions can be a tracer of the reflection symmetry breaking in the solar dynamo. It has required about twenty years of intensive efforts to obtain a more or less clear message for dynamo studies from observations of the current helicity observations (see e.g. Zhang et al. 2010). Currently, the nature of the the poloidal magnetic field on the Sun remains a matter of intensive discussions. In particular, solar dynamo models must assume fairly arbitrarily the value and form of the regeneration of poloidal magnetic field from toroidal, and the corresponding regeneration rate is a crucial governing parameter for the solar dynamo. Therefore, there is a fundamental interest in getting observational information concerning the induction mechanisms of the poloidal magnetic field in the solar dynamo, in order to learn which mechanism is most important.

An obvious relevant tracer here is the tilt angle of bipolar sunspot groups. As early as 1919 (Hale et al., 1919) Joy's law stated that that active sunspot regions tend to be "tilted", with the leading spot closer to the equator than the following spot. This law gives, quite straightforwardly, the desired link between toroidal and poloidal magnetic field. The importance of the Joy's law is that it gives the result of the combined action of all sources contributing to the desired link between toroidal and poloidal fields, while the other tracers (say, kinetic helicity) illuminate contributions of particular mechanisms to the joint result.

In spite of the fact that Joy's law is as old as the famous Hale polarity law, its impact on solar dynamo theory remained guite limited until recently, simply because the tilt angle data are much noisier than the sunspot polarity data. Recently, the accumulation of observational data and the progress of observational techniques, in particular due to the SOHO/MDI high resolution magnetograms, has provided sufficient data. This can be used to suppress the noise by averaging, and gives convincing results concerning Joy's law. In our opinion, the breakthrough was achieved in the fundamental paper by Stenflo & Kosovichev (2012), who convinced at least the solar dynamo community that the observations available allow the extraction of tilt angles with a reasonable level of confidence. Stenflo and Kosovichev (2012) presented tilt angle as a function of solar latitude averaged over the solar cycle. In general, their results look quite consistent with expectations from solar dynamo theory.

We believe that the available data enables us to make a further step and to clarify details of the temporal and latitudinal evolution of the tracers during the course of the solar cycle, as well as to learn the contribution in the tracer from bipolar sunspot groups of various intensities. The aim of this paper is to present the result of such an investigation, and to discuss it in the context of solar dynamos.

In presenting our results we exploit the standard methods in current helicity studies (Zhang et al. 2010), and obtain tilt angles averaged over latitudinal and temporal bins overlaid on the sunspot butterfly diagram. According to the current naive understanding of solar dynamo theory we do not expect to see in such a diagram any very dramatic behaviour of the averaged tilt angle. In this sense we confirm and extend the conclusion of Stenflo & Kosovichev (as well

as the earlier conclusion of Sivaraman et al. 1999) that the tilt angle does not vary dramatically during the course of the cycle. In contrast, we obtain, quite unexpectedly in the context of dynamo studies, that the tilt angle depends dramatically on the intensity of the bipolar group. Here we confirm and develop the preliminary conclusions of Tlatov and Obridko (2012). We present an interpretation of our results in the context of solar dynamo modelling.

#### 2 RECOGNIZING BIPOLAR GROUPS

We base our analysis on the magnetograms from Kitt Peak Vacuum telescope (KPVT), SOHO/MDI data (Scherrer et al, 1995; soi.stanford.edu/magnetic/Lev1.8/). In addition, we check the part of the obtained results by using fits files of 720-second cadence HMI data (Schou et al., 2012). Each magnetogram gives a map of the line-of-sight component of the magnetic flux density averaged over the spatial resolution window. We skipped from our analysis the magnetograms that have defected pixels (e.g., after the solar flares). The magnetograms that cover only part of the solar disk were skipped, as well.

Similar to Tlatov et al. (2010) and, also, Stenflo & Kosovichev (2012), we use a computer algorithm to isolate bipolar regions in solar magnetograms. The algorithm we use was suggested by Tlatov et al. (2010) and allows isolation of bipolar groups with low surface area or magnetic flux. This is why our data sample is richer than that analyzed by Stenflo & Kosovichev (2012), and it is essential in getting a tilt butterfly diagram. Stenflo & Kosovichev (2012) isolated about  $1.6 \times 10^5$  bipoles from about  $7.4 \times 10^4$  magnetograms, i.e. about 14 magnetograms per day, and so a rate of about 2 bipoles per day.

They considered active regions only. Because the lifetime of active regions substantially exceeds 1 day, the tilt information is redundant in that the tilt of a given bipole is measured many times. Our database for the same period 1996-2011 (MDI data) contains about  $6.8 \times 10^4$  bipoles from about  $4.5 \times 10^3$  magnetograms, i.e. 1 magnetogram per day, and so about 15 bipoles per day. For the period 1975-2003 (KPVT data – 3 cycles) we obtained about  $2.45 \times 10^5$  bipoles. To verify that these samples are not affected by noise or other known issues of MDI data (Liu and Norton, 2001) we used additionally HMI data (2010-2012), from which we obtained about  $9.7 \times 10^3$  bipoles (1 magnetogram per day). Apart from sunspot groups, our bipoles represent small ephemeral regions.

For the sake of consistency we recall here the basic elements of the algorithm suggested by Tlatov et al. (2010). The image with an example of the recognized bipolar groups can be found in the above cited paper

In Step 1, we look through the data set a for each magnetogram, we sift defective pixels do one nearest-neighbor smoothing (see Tlatov et al., 2010). Then, we select the monopole domains with magnetic field exceeding the threshold level  $B_{\rm min}$  for positive and negative values of  $B_{\rm min}$  separately. For each connected domain the following parameters are then calculated: the heliographic coordinates of the geometrical center of the domain including the projection effect, its area measured in millionths of the solar

hemisphere  $(MSH^1)$ , and the magnetic flux through this area.

The next stage is to search for a domain of given polarity (domain 1) and a corresponding domain (domain 2) of the opposite polarity. We sift the structures with area less than 20 MSH from the search The search is performed in a circular region whose center is located at the geometrical center of the initial domain and with radius  $7^{\circ} + dL/2$  on the solar disc, where dL is a longitudinal size of this domain. Note that the value of  $7^{\circ}$  corresponds to the mean distance between pores in bipolar sunspot groups of the Zürich Class B (Vitinsky et al., 1986). It looks reasonable to introduce a criterion that both domains have more or less equal magnetic fluxes, i.e.  $||F_1| - |F_2||/(|F_1| + |F_2|) < \varepsilon$ , and to require that that the distance between the corresponding domains is minimal. Each search is started with an arbitrary pole of positive polarity. For this element the program finds the best neighbor match for the negative polarity pole. After this, a reverse search is performed to find the closest neighbor for the negative pole. If the search returns the same pair of negative and positive poles, the pair is marked and is taken out of the next search. The search was restricted to the central zone, within  $\pm 60^{\circ}$  from the central meridian of solar disc.

Finally, we calculate the tilt angle  $\mu$  as the angle between a line connecting the geometrical centre of the domain with the negative polarity with the centre of the domain with positive polarity in a bipolar group, and the solar equator. We associate the tilt with the bisecting point of this line. If the leading polarity is positive the tilt is close to  $0^{\circ}$  while if the leading polarity is negative the tilt is near  $180^{\circ}$ .

Tlatov et al. (2010) demonstrated that the algorithm is quite robust. Examples of the identified bipoles are given in Fig. 1. Of course, it can sometimes give identifications that look irrelevant, especially for small bipoles. However the main statistical properties seem reliable to within a general level of noise. Basically we used one magnetogram per day, but for the MDI data set we made an additional check with 7 magnetogram per day and find the same results (within the level of noise). The given results were confirmed by the procedure where the search domain was restricted to the central zone within  $\pm 30^{\circ}$  from the central meridian of the solar disc. These support the conclusion about robustness of the principal algorithm.

As opposed to Stenflo & Kosovichev (2012) we used significantly lower smoothing and lower values of threshold levels for magnetic field. We obtained individual substantive domains with appropriate coordinates and fluxes. It allow us to perform an analysis for substantially smaller structures versus Stenflo & Kosovichev (2012). There are also some differences in determination of tilt angle. We calculate tilt between two domains with similar fluxes rather then between geometric averaged fields with different directions that usually consist of many unconnected regions inside the box used by Stenflo & Kosovichev (2012).

Additional information obtained during the

Selection criteria	KPVT	MDI	HMI
50 < S < 300  MHS	$201\ 221 \\ 44\ 821$	50 195	6754
S > 300  MHS		18 096	2911

Table 1. The number of bipoles in the database investigated

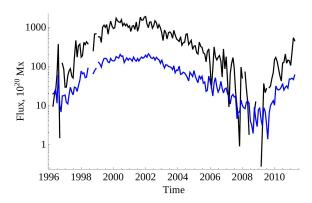


Figure 2. The flux according to MDI data. The black line corresponds to areas S>300 MSH, blue line shows the total flux from bipoles with areas 50 < S < 300 MSH.

identification of the groups allows separation of groups of given ranges of areas.

Obviously, it is useful for the analysis to obtain as many bipoles as possible. On the other hand, as more bipoles are collected weaker bipoles have to be included in the database. We recognize that it is difficult to determine mean tilt for weak bipoles, because the tilt angle distribution is almost homogeneous. We expect, and confirm the expectation by the following analysis, that some features of bipole distribution become unstable if the weakest bipoles are included. Therefore we set a lower limit on the area of bipoles - they should exceed 50 MSH. Smaller bipoles require more sophisticated analysis. Below we grade the results obtained with respect to the level of their stability according to various selection criteria applied. Some statistical data concerning database used are given in Table 1.

Fig. 2 presents graphics of total flux according to MDI data for small (50 < S < 300 MSH) and large (S > 300 MSH) bipolar groups. The lower bound S = 50 MSH is chosen because the tilt angle distribution becomes practically homogeneous for smaller bipoles. The bounding value S = 300 MSH is chosen because the tilt angle properties are more or less stable for larger bipoles. Another important point here is that the size of such bipoles more or less corresponds to the super-granulation scale. We see that both small and large bipoles are involved in the solar cycle. Of course, the contribution from small bipoles to the total magnetic flux is substantially smaller than that from the large bipoles.

We demonstrate the correctness of our selection of small and large bipolar groups as follows. According to the Hale polarity law the sunspot groups have opposite leading polarity in successive cycles in one hemisphere, as well as between hemispheres in a single cycle. Fig. 3 confirms this symmetry for small bipoles and shows that the wings of the butterfly diagram which separate regions of the opposite

 $<sup>^1~</sup>$  1 MSH = 3.044  $\times$  10  $^6~$  km². The round shaped spot with area S (in MSH) has a diameter  $d=1969\sqrt{S}~$  km =  $(0.1621\sqrt{S})^{\circ}.$  See Vitinsky et al., 1986.

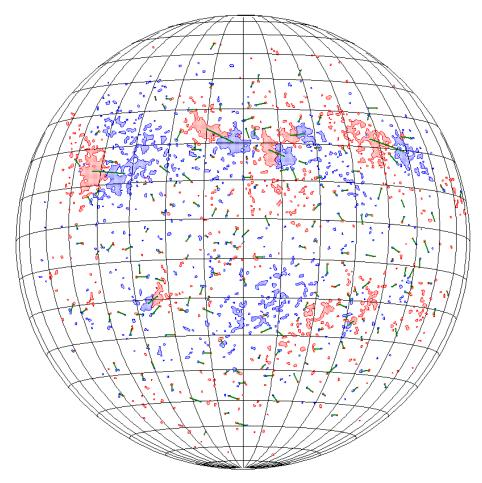
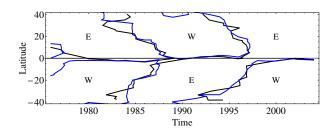


Figure 1. Examples of bipole identification at MDI magnetogram from 2011 April 11.



**Figure 3.** Illustrating the prevalent E-W direction of tilt according to KPVT. Black shows areas S>300 MSH, blue the areas 50 < S < 300 MSH.  $B_{\rm min}=10$  G.

sign almost coincide for large and small bipoles: black lines separate areas with prevalent number of large bipolar groups ( $S>300~\mathrm{MSH}$ ) in east or west direction. The blue lines separate the same areas for smaller bipolar groups ( $50 < S < 300~\mathrm{MSH}$ ). We consider the fact that the areas separated by blue lines are quite similar to the areas separated by black lines as a confirmation of correctness of our selection.

#### 3 AVERAGING TILT

Obviously, the tilt for a given bipolar region is a quite noisy quantity and we are interested in the tilt data averaged over suitable latitudinal and temporal intervals. For averaging we use 2-year time bins and  $5^{\circ}$  latitudinal bins and then consider the data for a given activity cycle as required. An example of the tilt angle distribution for a given time-latitude bin is shown in Fig. 4.

In averaging the distribution we have to take into account that the method applied to measure the tilt can give rare and strong non-Gaussian deviations from the mean. For example, a bipolar group with inverse polarity which violates the Hale polarity law gives by definition a derived tilt which differs from its true value by  $180^{\circ}$ . This happens only in about 5% of cases (e.g. Sokoloff and Khlystova, 2010). The relative number of small bipoles that violate the polarity law is larger than that for sunspot groups, about 10-20% and they quite usually give an additional maximum in the tilt angle distribution, displaced from the primary by  $180^{\circ}$ . However the tilt is usually quite close to  $0^{\circ}$  or  $180^{\circ}$  and we discard rare and strong non-Gaussian deviations.

We perform this averaging as follows. In the first step, we select for a given bin a hemisphere, either East (tilts  $-90^{\circ} < \mu < +90^{\circ}$ ) or West (tilts  $90^{\circ} < \mu < 270^{\circ}$ ), from where the tilt data are taken for averaging. We approximate the tilt distribution in each hemisphere by the Gaussian  $\frac{A}{\sigma} \exp(-(x-a)^2/\sigma^2)$ , where A is an amplitude, a is a mean, and  $\sigma$  is a standard deviation, and choose the hemisphere where A is larger. As a rule this means that the number of tilts which are directed in this hemisphere is larger than

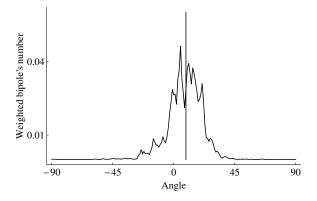


**Figure 4.** An example of the tilt distribution for the MDI data (for 2001 - 2002) at  $12.5^{\circ} \leq \theta \leq 17.5^{\circ}$  for areas S > 300 MSH (weighted data). The vertical line indicates the median of sample. Graphic is normalized to unit square.

directed in the opposite hemisphere. If desirable, we can weight the data using, say, the areas of the bipoles.

In the second step we apply the robust statistical measure (median) to estimate the desired mean value and corresponding uncertainties. We order the tilt angles from the bin as  $\mu_1 \leq \mu_2 \leq \ldots \leq \mu_n$ , i=1...n and take  $\mu_{((n+1)/2)}$  as the averaged quantity m for the tilt if n is odd and  $\frac{1}{2}(\mu_{(n/2)} + \mu_{(n/2+1)})$ , if n is even. For large n the estimate becomes Gaussian with mean m and standard deviation  $\sqrt{\pi \frac{1}{n-1} \sum (\mu_i - m)^2}$  and then we can estimate uncertainties using the standard Student criterion with n-1 degree of freedom (see Huber 1981).

Note that the number of large bipoles in our sample decreases sharply with the growth of bipole area. In order to increase the contribution of the largest bipoles (including sunspots) to the average we use weighting. Small bipoles largely determine the non-weighted averaging. We define the tilt as being positive if it is clockwise and negative if counterclockwise, regardless of hemisphere.

#### 4 RESULTS

## 4.1 Joy's law

We start our analysis by verifying the results of Stenflo & Kosovichev (2012) for our sample, assuming that the tilts scale with co-latitude as  $k \sin \theta$ .

In Fig. 5 we present the averaged tilts for the MDI data for 1996–2011 with combined northern and southern hemispheres, following the presentation of the data by Stenflo & Kosovichev (2012). We selected the bipoles with the minimal magnetic field limit  $B_{\rm min}=10~{\rm G}$  and took those with area  $>300~{\rm MSH}$ . The data are weighted according to the bipole areas. We see from Fig. 5 that Joy's law is in the form discussed by Stenflo & Kosovichev (2012), except for the smaller inclination of the fitted curve because of the bending of Joy's law at 30° (the bending is absent in Stenflo & Kosovichev, 2012 plots and the nature of the bending deserves a further clarification).

The correlation changes dramatically when smaller bipoles are taken into account. We can see from Fig. 6 that bipoles with areas 50-300 MSH possess the opposite sign

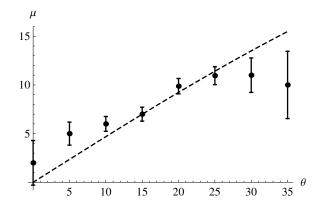
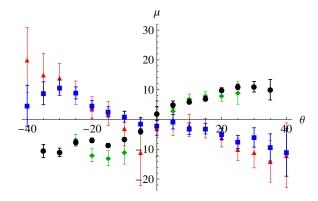


Figure 5. Joy's law for MDI data, bipoles with the minimal magnetic field limit  $B_{\rm min}=10$  G, area S>300 MSH. The error bars indicate 95% confidence interval. The dashed curve is the fit function  $\mu=27\sin\pi\theta/180^\circ$ .



**Figure 6.** Joy's law according to MDI and HMI data. Black squares correspond to areas S>300 MSH for MDI, green diamonds – to areas S>300 MSH for HMI. Blue points correspond to areas 50< S<300 MSH for MDI, red triangles – to areas 50< S<100 MSH for HMI. 50 HMI. 50 MSH for MDI and 50 MSH for HMI.

of tilt. This average for small bipoles is not weighted. Note that, as for the large bipoles, there is a slight bending in Joy's law for small bipoles at latitude  $30^{\circ} - 40^{\circ}$ .

We obtain that the analysis of HMI data confirms the above obtained unusual behaviour of small bipoles. The short period covered with HMI (2010-2012) does not allow us to make detailed estimations, but at qualitative level we can see from Fig. 6 that small bipoles also have the inverse Joy's law. The thresholds  $B_{\rm min}$  and S for HMI were shifted to keep daily number of bipoles comparable to MDI sample over a period of its simultaneous work (2010-2011).

We verify the above conclusions about the bipoles from a longer period of observation (KPVT data, 1975-2003, i.e.3 cycles),  $B_{\rm min}=10$  G (Fig. 7). We see from Figs. 7 and 6 that the absolute value of tilt for small bipoles rises continuously from the equator to middle latitudes (inverse Joy's law).

Note that the available data allow derivation of the correlations for cycles 21, 22 and 23 separately and confirm that the value k does not vary substantially from one cycle to the next, see Fig. 8. We do not observe such variations for cycles 23 and 24 as well (Fig. 6). Our interpretation is

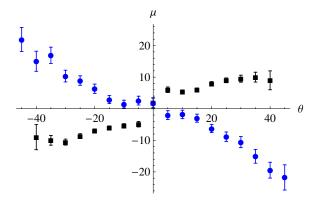


**Figure 7.** Joy's law for KPVT,  $B_{\rm min}=10$  G; black squares correspond to areas S>300 MSH, blue points correspond to 50 < S < 300 MSH.

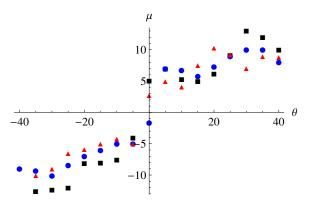


**Figure 8.** Joy's law according to the weighted KPVT data,  $B_{\rm min}=10$  G, area S>300 MSH. Black squares - cycle 21, blue circles - cycle 22, red triangles - cycle 23.

that the weighting suppresses efficiently the impact of small bipoles.

Obviously, tilt can depend not only on area, but also on the strength of the magnetic field. To check this we made a selection taking  $B_{\rm min}=100$  G for the KPVT data. Fig. 9 shows that tilts for small bipoles (<100 MSH) have the opposite sign, but with lower value than for the larger bipoles.

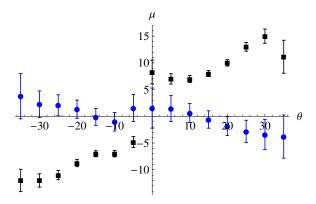


**Figure 9.** Joy's law for KPVT,  $B_{\rm min}=100$  G, black squares correspond to areas >100 MSH (weighted tilts), blue points to areas S<100 MSH (non-weighted tilts).

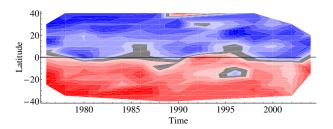


Figure 12. Butterfly diagram for tilt alone according to KPVT. Blue is for positive tilt, red is for negative tilt, grey is used to indicate areas where the tilt is zero to within the confidence intervals.  $B_{\rm min}=10$  G, areas S>300 MSH.

## 4.2 Butterfly diagram: tilt data and sunspot data

We move now to the space-time distribution of the averaged tilt angle data overlaid on the sunspot butterfly diagram. As we learn from the above analysis of Joy's law, we have to consider contributions from large and small bipoles separately, using an appropriate selection and weighting procedure.

Fig. 10 shows the distribution for the MDI data for sunspots, cycle 23. We see from the Figure that an averaged positive tilt is strongly preferred in the Northern hemisphere, while negative tilt is strongly preferred in the Southern. A few minor exceptions from this polarity rule can be seen at the very end of the cycle and near the solar equator. Exceptions for a corresponding polarity rule are known as well for the current helicity data, e.g. Zhang et al. (2010).

Fig. 11 shows that the polarity rule for the tilt is reversed if we consider only the contribution of the small bipoles.

### 4.3 Butterfly diagram: tilt data

The next figures present the time-latitude distribution of the tilt data alone by colours: blue means positive tilt and red negative tilt; whereas gray means that the tilt is zero to within the confidence intervals. We see in Fig. 12 that the tilt is mainly positive in the North hemisphere and mainly negative in the South hemisphere. Some exceptions from this polarity rule are associated mainly with the areas between cycles. Equatorward propagating patterns are weak but still visible inside the cycles. In places they have a double-peak structure: maxima are located at the beginning of the cycle at higher latitudes and at the end of the cycle at lower latitudes.

By increasing the lower limit  $B_{\rm min}$  to 100 G equatorward propagating patterns, connected with cycles, almost disappear. In Fig. 12 and Fig. 13 we have used a weighting to increase the contribution of the largest domains, which include sunspots. We confirm that the tilt for large bipolar groups at given latitude does not vary substantially (Fig. 13).

The corresponding picture for small bipoles gives, as expected, the inverse color distribution. In Fig. 14 we see well defined equatorward propagating waves indicating that the small bipoles are involved in the solar cycle and give a butterfly diagram similar to that obtained from the sunspot data. Note however, that these waves seem to begin at higher

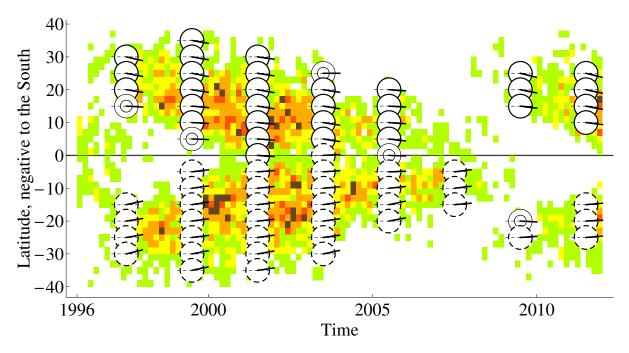


Figure 10. Showing the butterfly diagram (tilt data overlaid sunspot data) for cycle 23, from weighted MDI data,  $B_{\min} = 10$  G, areas S > 300 MSH. The tilt angles are shown as circles. Solid circles correspond to the bins with positive mean value of the tilt angle and zero tilt does not belong to the confidence intervals for this mean value. Dashed circles correspond to the bins with negative mean value of the mean value of the tilt angle and zero tilt does not belong to the confidence intervals for this mean value. Double circles stand for the bins where zero tilt belongs to the confidence intervals. Note that tilt is positive if the tilt is clockwise and negative if the tilt is counterclockwise regardless of hemisphere.

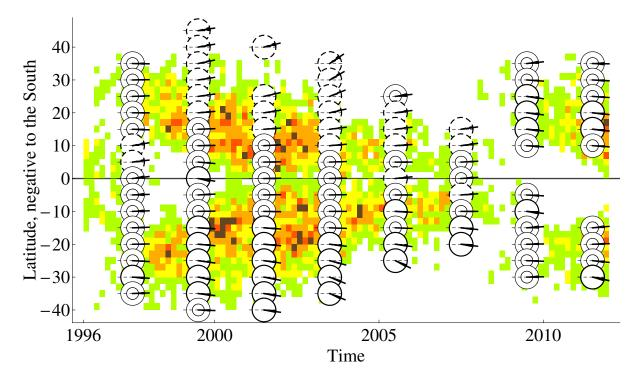


Figure 11. Butterfly diagram (tilt data overlay sunspot data) for cycle 23, non-weighted MDI data,  $B_{\min} = 10$  G, areas 50 < S < 300 MSH. Notation as in the previous figure.

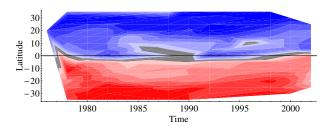
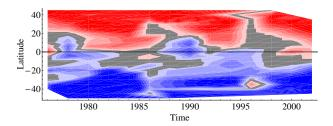


Figure 13. Butterfly diagram for tilt alone according to KPVT.  $B_{\min}=100$  G, areas S>100 MSH. The color notation as in previous figure.



**Figure 14.** Butterfly diagram for tilt alone according to KPVT.  $B_{\min} = 10$  G, areas 50 < S < 300 MSH. The color notation as in previous figure.

latitudes compared with waves from sunspots. This could be an indication of the so-called "extended solar cycle".

## 5 DISCUSSION

We have demonstrated that the method for isolation of bipoles suggested by Tlatov et al. (2010) provides sufficient data to address the time-latitude distribution of the tilt angle in detail and to obtain Joy's law for particular time-latitude ranges. In this sense our results generalize the results obtained by Stenflo & Kosovichev (2012).

We found that the tilt angle averaged over suitable timelatitude bins is distributed antisymmetrically with respect to the solar equator. As far as we can follow the latitude distribution, the absolute value of the tilt angle is larger for larger latitudes.

Quite unexpectedly, we obtained that the results depend on the size of bipoles included in the investigation, i.e. the large bipoles with S>300 MHS (which are mainly sunspot groups) and small bipoles with 50 < S < 300 MHS (which are mainly ephemeral regions) give significantly different results concerning the tilt angle behaviour. The results for large bipoles look much more significant and easy to interpret than those for the small bipoles. In particular, the results here agree (at least qualitatively) with the results obtained by Stenflo & Kosovichev (2012). We find that the tilt angle is positive in the Northern hemisphere and negative in the Southern.

Note however that we obtain a smaller inclination factor when the fitting the tilt data as being proportional to  $\mu = a \sin \pi \theta / 180^{\circ}$ . We obtained  $a = 27 \pm 4$  ( $2\sigma$  error bar is given) while Stenflo & Kosovichev(2012) suggest a = 32. We believe that the discrepancy between the data analyses reflects the fact that the databases used are specifically biased by smaller bipoles. In other words, the formal statistical

uncertainties shown in the figures do not take into account a possible bias from the small bipoles. Of course, this possible bias constrains recognition of various features found in the tilt butterfly diagrams.

The results presented on Figures 10-14 are new and they generalize the previous findings (see, Tlatov et al, 2010; Stenflo & Kosovichev, 2012) giving information about the time-latitude variation of the tilt angle for the bipolar regions of different size. It was found that the tilt angle distribution remains stable showing no substantial variations from one cycle to another. For the large bipoles the variations in the tilt angle which occur during a given solar cycle mainly reflect the propagation of the activity wave to the equator. It is found that for the large bipoles the average sign of the tilt in the given hemisphere is preserved for the separated cycles. This is different from what is observed in the time-latitude distribution for the current helicity (Zhang et al. 2010).

Solar dynamo theories include a physical link between toroidal and poloidal solar magnetic field, which results in a non-vanishing tilt. The nature of this link is specific for any particular dynamo scenario. In the Parker (1955) scenario it is a result of the  $\alpha$ -effect arising from the mirror-asymmetric solar convection, while the Babcock-Leighton scenario (Babcock, 1961, Leighton, 1961) exploits a direct action of the Coriolis force on the rising magnetic loop. This can be interpreted as a nonlocal  $\alpha$ -effect. The direct numerical simulations by Brandenburg (2005) suggest another possibility. His results suggest that near the solar surface the  $\alpha$ -effect can be dominated by effects of the shear, and the tilt angle is a result of the latitudinal differential rotation. Except for the mechanisms mentioned above, both mean-field theory and direct numerical simulations suggests the existence of additional induction effects of the turbulence, which could transform the toroidal magnetic field to poloidal and vice versa. The  $\Omega \times J$  effect (Rädler, 1969) – also called the  $\delta$ -effect – originates from the Coriolis force acting on the current, and is induced by the turbulent magnetic field linked with the large-scale field (see, e.g., Pipin & Seehafer 2009). Direct numerical simulations confirm the importance of the  $\delta$ -effect as well as the  $\alpha^2$ effect for the global dynamo in the convective zone of a star (Käpylä et al 2008, 2009; Schrinner et al 2011, 2012).

Of course, details of the time-latitude distribution of the tilt depend on particular features of the model and the scenario as a whole. It looks plausible that the tilt data can help to determine which scenario or combinations fits the true solar activity better (e.g. Dasi-Espuig (2010) claim that the tilt data support the Babcock-Leighton scenario). Our feeling is that a final decision here needs extensive numerical modelling in light of the tilt data obtained, and so we reserve our opinion here and use below the notation  $\alpha$  as a common notation for the link between toroidal and poloidal magnetic fields in either picture.

From the viewpoint of dynamo theory, the tilt data can be considered as a direct observational determination of the principal drivers in solar dynamo, i.e. the  $\alpha$ -effect (or, more carefully, of a mirror-asymmetric driver responsible for conversion of toroidal magnetic field to the poloidal). Our results confirm the basic expectations of dynamo models concerning properties of  $\alpha$ . The quantity is antisymmetric in respect to the equator, it increases with latitude and

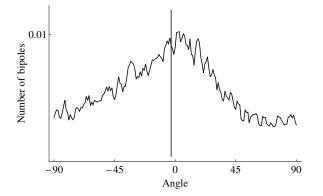


**Figure 15.** Tilt distribution for MDI data (for 1996 - 2011) at  $12.5^{\circ} \leq \theta \leq 17.5^{\circ}$  for areas 50 < S < 300 MSH (non-weighted data). Vertical line indicates median of sample. Graphic is normalized to unit square.

does not demonstrate pronounced cycle-to-cycle variations. Some variations of  $\alpha$  within the cycle can be attributed to nonlinear suppression of dynamo action. Note, theoretical calculations (see, e.g., Fig.1e in Pipin & Kosovichev 2011) as well as direct numerical simulations (e.g., Käpylä et al. 2006, 2008) show that  $\alpha$  is positive in the Northern hemisphere in most of the convection zone. It changes sign to become negative near the bottom of the convection zone.

We can estimate the absolute value of  $\alpha$  as follows. The typical tilt does not exceed  $\mu=10^\circ$  – about 10% of the extent of the first quadrant,  $0^\circ < \mu < 90^\circ$ , where the tilt of the given sign can, principle, vary. If we identify the life time of bipoles with the convection turnover time and suggest that a convective vortex performs a full rotation during the turnover time, we find that  $\alpha \approx 0.1v$  where v is the r.m.s. convective velocity. A more accurate estimate requires detailed numerical modelling and is constrained by the bias discussed above; however the range of  $\alpha$  obtained looks consistent with the concepts of dynamo theory.

In any case we can conclude that  $\alpha$  is no longer just a theoretical concept supported only by theoretical findings, but has now a direct observational confirmation. Our results do not clarify the physical nature of  $\alpha$  directly, but further modelling of the dynamo based on the data obtained in the framework of other relevant data can, in principle, help to decide a relevant option. Such modelling however is obviously out of the scope of this paper.

The tilt data associated with small bipoles show that these have a sign of tilt which is opposite to the tilt sign derived from the data for large bipoles. Comparing the distribution of the tilts of the small bipoles shown in Fig.s 15 and 16 we conclude that the origin of the negative tilt is different at low and high latitudes.

In fact, at low ( $< 30^{\circ}$ ) latitudes the negative tilt is caused not by the sign of the maximum of the distribution, but by the more populated tail of the distribution. We can interpret this as a mixture of two populations. This is different to results by Stenflo & Kosovichev(2012), who found that small bipoles follows to the standard Joy's law being oriented in the same direction as the sunspots. One is located in the area of positive angles (standard bipoles) and defines the maximum of the distribution, whereas another is located in the area of negative angles and shifts the mean

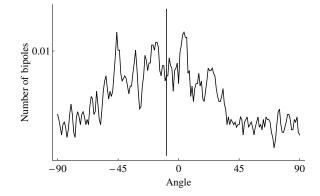


Figure 16. Tilt distribution for MDI data (for 1996 - 2011) at  $32.5^{\circ} \le \theta \le 37.5^{\circ}$ , and areas 50 < S < 300 MSH.

tilt. At higher latitudes ( $>30^{\circ}$ ) the number of standard bipoles with positive tilts (which are supposed to trace the toroidal magnetic field) decreases and we see the prevalent component with negative tilt. These results complement the study by Tlatov et al. (2010) who found that the size of population of the oriented small bipoles starts to grow at the latitudes larger than  $20^{\circ}$  just after the solar maximum having the polar and equatorial branches of activity. It was claimed that this support an idea about an extended solar cycle. We can speculate about another possibility.

Extending the idea given by Brandenburg (2005), we can assume, that at higher latitudes we observe tracers of poloidal component of the solar magnetic field that is converted by the  $\alpha^2$  mechanism into the toroidal field. Indeed, such bipoles, being initially oriented in the meridional direction, can obtain negative tilts from to the action of the Coriolis force. For meridionally oriented bipoles the Coriolis force is minimal near the equator and maximal near the poles, hence the tilt should decrease towards the poles and we should again see Joy's law. We can see such behaviour in Fig. 6, where the curve of Joy's law has a visible bend at  $\theta=-30^\circ$ . Of course, other mechanisms, for instance differential rotation, can affect the tilt distribution and cause difficulties for the sign determination, especially at lower latitudes.

We appreciate that the criteria for bipole definition and averaging can be varied to some extent. These variations affect the tilt distribution of the larger dipoles more weakly than for the smaller. We used median as a robust statistic and Student criteria for confidence intervals. This method confirmed the first estimations in Tlatov et al. 2010. However we failed to find a convincing scheme of data processing which would give positive tilt for the small bipoles in the Northern hemisphere. The choice of criteria which we used to obtain the the above results is one of the most severe in respect to obtaining a negative tilt of small bipoles in the Northern hemisphere. This conclusion is supported by consideration of the newest observational data provided by HMI.

Our findings can be summarized as follows. For bipoles with larger area, the tilt angle is positive in the Northern hemisphere and negative in the Southern, with a latitudinal profile proportional to  $\cos \theta$ . In comparing our results with those by Tlatov et al. (2010) we found that the bipoles with smaller area are non-homogeneous and can be decomposed

10

into two populations. One of them is associated with the bipoles that follow the standard tilt angle law and contains mostly sunspots at the early stages of their evolution. Another group is constituted mainly of the ephemeral regions and has a tilt angle which is of opposite sign to the tilt of the bipoles of larger area. The tilt of bipoles of the second group is produced by specific mechanisms, and some possible explanations have been discussed above. The ratio between two groups depends on the latitude zone considered. At low latitudes bipoles of the first group dominate, but the second group provides a heavy tail to the tilt distribution. At high latitudes the number of sunspots vanishes and the second group dominates. Extending the results of the previous studies (see, Tlatov et al, 2010; Stenflo & Kosovichev, 2012; and by Tlatov & Obridko, 2012) we found that the tilt angle distribution remains stable showing no substantial variations from one cycle to another.

Finally, we summarize what is the new message from our paper to dynamo theory in comparison to that one from Stenflo & Kosovichev, 2012. We focus the attention on the variations tilt angle distribution in course of a given cycle to found that this distribution remains rather stable and deviations from this general distribution are quite small and local. In this respect, tilt angle differs substantially from the current helicity which traces mirror asymmetry of magnetic field (Zhang et al., 2010). This simple behaviour of the tilt means that the simple models of solar dynamo based on primitive parameterization of the regeneration rate of poloidal magnetic field from toroidal one and simple phenomenological algebraic quenching of this regeneration rate reproduce rather well the true phenomenology. Of course, such models do not clarify physical mechanisms underlying the phenomenon however provide a reasonable pragmatic approach to its description. We believe that the tilt angle data presented can be used in order to improve such simplified models for stellar dynamos and historical reconstructions of solar activity. In principle, we would be happy to achieve this limited however important goal. In fact however we isolated an unusual behaviour of small bipoles. We explain it as a manifestation of regeneration of toroidal magnetic field from poloidal one due to the mirror asymmetric effects in solar dynamo. If this interpretation will be supported by future investigations, it will give a completely new source of observational information concerning governing parameters of solar dynamo.

We stress that an independent verification of the results concerning small bipoles by other methods of bipole recognition is highly desirable before a dynamo interpretation of this result can be robustly supported or rejected.

#### Acknowledgements

The paper is supported by RFBR under grants 13-02-91158 (AT, EI), 12-02-00614 (AT), 12-02-31128 (EI), 12-02-00884 (EI), 12-02-00170 (EI, DS, VP). We are grateful to J.Stenflo and D.Moss for a critical reading of the manuscript, and helpful comments.

#### REFERENCES

Babcock, H.W., 1961, ApJ, 133, 572

Brandenburg, A., 2005, ApJ, 625, 539

Choudhuri, A.R., Schüssler, M., Dikpati, M., 1995, A&A, 303, L29 Dasi-Espuig, M., Solanki, S.K., Krivova, N.A., Cameron, R., Penuela, T., 2010, A&A, 518, A7

Dikpati, M., Charbonneau, P., 1999, ApJ, 518, 508

Dikpati, M., Gilman, P.A., 2001, ApJ, 559, 428

Hale G.E., Ellerman, F., Nicholson, S.B., Joy, A.H., 1919, ApJ, 48, 153

Huber P.J., Robust Statistics, 1981, Wiley

Käpylä, P. J., Korpi, M. J., & Brandenburg, A. 2008, A&A, 491, 353

Käpylä, P.J., Korpi, M.J., Ossendrijver, M. and Stix, M., 2006, A&A, 455,401–412

Krause, F., Rädler, K.-H., Mean-field magnetohydrodynamics and dynamo theory, 1980, Pergamon, Oxford

Leighton, R.B., 1969, ApJ, 156, 1

Liu, Y., Norton, A.A. 2011, SOI-Technical Note 01-144

Parker, E.N., 1955, ApJ, 122, 293

Pipin, V.V., Kosovichev, A.G., 2011, ApJ,738,104

Pipin, V.V., Seehafer, N., 2009, A& A, 493, 819

Rädler, K.-H. 1969, Monatsber. Dtsch. Akad. Wiss. Berlin, 11, 194, in German, English translation in ed. P. H. Roberts, & M. Stix, Report No. NCAR-TN/IA-60 (1971)

Scherrer, P. H., et al. 1995, Solar Phys., 162, 129

Schou, J., Scherrer P.H., Bush, R.I., Wachter, R., Couvidat, S., Rabello-Soares M.C., Bogart R.S., Hoeksema J.T., Liu, Y., Duvall, T.L., Akin, D.J., Allard, B.A., Miles, J.W., Rairden, R., Shine, R.A., Tarbell, T.D., Title, A.M., Wolfson, C.J., Elmore, D.F., Norton, A.A., Tomczyk, S., 2012, Solar Phys., 275, 229

Schrinner, M., Petitdemange, L., & Dormy, E., 2011, A&A, 530, A410

Schrinner, M., Petitdemange, L., & Dormy, E., 2012, ApJ, 752, 121

Seehafer, N. 1990, Sol. Phys, 125, 219

Sivaraman, K. R., Gupta, S.S., Howard, Robert F., 1999, Solar Phys., 189, 69

Sokoloff, D., Khlystova, A.I., 2010, Astron. Nachr., 331, 82

Stenflo, J.O., Kosovichev, A.G., 2012, ApJ, 745, 129

Tlatov A.G., Obridko V.N., 2012, In: Comparative Magnetic Minima: Characterizing quiet times in the Sun and stars, IAU Symp. 286, D. Webb & C. Mandrini (eds), Cambridge, 113

 Tlatov, A.G., Vasil'eva, V.V., Pevtsov, A.A., 2010, ApJ, 717, 357
Vitinsky, Yu.I., Kopecky, M., Kuklin, G.V., 1986, Statistics of the Sunspot Activity, Nauka, Moscow

Zhang, H., Sakurai, T., Pevtsov, A., Gao, Yu, Xu, Haiqing, Sokoloff, D.D., Kuzanyan, K., 2010, MNRAS, 402, L30